The South Pacific Current

LOTHAR STRAMMA

Institut für Meereskunde an der Universität Kiel, Kiel, Germany

RAY G. PETERSON

Scripps Institution of Oceanography, University of California, San Diego, La Jolla, California

MATTHIAS TOMCZAK

Flinders Institute of Atmospheric and Marine Sciences, The Flinders University of South Australia, Adelaide, South Australia, Australia

(Manuscript received 23 February 1993, in final form 9 May 1994)

ABSTRACT

The Southern Hemisphere Subtropical Front (STF) is a narrow zone of transition between upper-level subtropical waters to the north and subantarctic waters to the south. It is found near 40°S across the South Atlantic and South Indian Oceans and is associated with an eastward geostrophic current band. The current band in each basin is found at or just north of the surface front except near the eastern boundaries where most of the subtropical waters turn north into the eastern limbs of the subtropical gyres. The bands associated with the STF are thus distinct features separated from the strong zonal flows of the Antarctic Circumpolar Current farther south. The authors have referred to the current bands in the two respective oceans as the South Atlantic Current and the South Indian Ocean Current. In this paper the authors use the historical database from the South Pacific Ocean to investigate the geostrophic flow associated with the STF there. The STF extends across the southern Tasman Sea from south of Tasmania to southern New Zealand, and a weak eastward flow appears to be associated with it. The transport amounts to only about 3 Sv (1Sv $\equiv 10^6$ m^3 s^{-1}), little of which passes south of New Zealand. Mixing within the eddy-rich Tasman Sea may account for this weakness, while also setting up another more significant front in the northern Tasman Sea, the Tasman Front. It branches off from the East Australian Current toward the north of New Zealand, along which moves a flow of about 14 Sv. After passing north of New Zealand, a portion of this current flows east to contribute to a current band near 30°S, while another portion turns south as the East Auckland Current and meets with subantarctic waters near Chatham Rise (44°S), thus reestablishing the STF.

An enhanced eastward current band is associated with the front there, one that extends across the remainder of the South Pacific and is referred to as the South Pacific Current. In comparison with its counterparts in the other basins, which typically begin by carrying 30 Sv (Atlantic) to 60 Sv (Indian) in the upper 1000 m in their western portions before weakening to 10–15 Sv in the east, the South Pacific Current is weak. Near Chatham Rise, it starts with a transport of approximately 5 Sv, and it remains near this strength as it shifts gradually north across the basin toward South America. The current appears to split into two smaller bands in the region of 115°–85°W, while near 28°S, 83°W it begins to turn more strongly north and becomes shallower and weaker. Potential vorticity distributions indicate that this current acts as an impediment toward the northward spreading of Antarctic Intermediate Water. But why the South Pacific Current east of New Zealand should be so much weaker than its counterparts in the other basins is not particularly clear. It may be due to the presence of New Zealand and other topographic barriers to deep flow east of Australia, to the axis of the subtropical gyre in the South Pacific shifting more rapidly southward with depth than those elsewhere, thus causing greater reductions in the underlying zonal velocities, and to strong poleward eddy heat and salt fluxes in the other two basins leading to smaller cross-STF gradients in the Pacific.

1. Introduction

The subtropical and midlatitude oceans in the Southern Hemisphere are acted upon by positive mean wind stress curl, which drives downward Ekman pumping; hence, the term "subtropical convergence" is sometimes applied to this broad oceanic domain. In the South Pacific it occupies the zone lying between approximately 20° and 50°S. The subtropical convergence described by Deacon (1933, 1937), on the other hand, is a relatively narrow band within this zone where enhanced meridional temperature and salinity gradients exist in the upper-level waters. This convergence, which marks the transition between warm and saline subtropical waters to the north and cool relatively fresh subantarctic

Corresponding author address: Dr. Lothar Stramma, Institut fuer Meereskunde, Duesternbrooker Weg 20, 24105 Kiel, Germany.

© 1995 American Meteorological Society

waters to the south, is now frequently referred to as the "Subtropical Front" (STF).

The STF is nearly continuous in the Southern Hemisphere. It begins in the South Atlantic at the confluence of the Brazil and Falkland (Malvinas) Currents and extends eastward across that ocean and the southern Indian Ocean at latitudes ~35°–45°S. It passes south of Australia and Tasmania, and once past New Zealand the STF continues across the South Pacific before turning northward off the west coast of South America to diffuse in lower latitudes. Because the meridional temperature and salinity gradients across the front have the same sign, they have opposing effects on density. In both Atlantic and Indian Oceans, changes in temperature are more influential on density, and as a consequence, a narrow eastward current band is found at or just north of the surface front. We have referred to this current band, in its respective oceans, as the South Atlantic Current (Stramma and Peterson 1990) and the South Indian Ocean Current (Stramma 1992). In the western portions of their basins, these two currents typically carry 30 (Atlantic) to 60 (Indian) Sv (1 Sv $\equiv 10^6$ m^3 s^{-1}) in the upper 1000 m, while in the eastern portions their transports diminish to 10–15 Sv. These current bands are distinctly separated from the strong zonal flows of the Antarctic Circumpolar Current by a region of relatively weak flow, the Subantarctic Zone, and they each become at least partially disjoined from the STF when they turn north in the eastern portions of their basins to close the subtropical gyre circulations.

The purpose of this paper is to determine if there is an identifiable current band associated with the South Pacific STF and, if so, how it compares with those in the South Atlantic and South Indian Oceans. We do this with a number of quasi-synoptic sections made in the region between Australia and Chile. We find that such a current band does exist, though it is significantly weaker than in the other two basins. The flow associated with the STF in the Tasman Sea does not appear to be continuous with that in the remainder of the South Pacific, so the term "South Pacific Current" is used here for only the flow east of New Zealand. New Zealand is often considered to be the western boundary for the subtropical recirculation south of 35°S (e.g., McCartney 1982).

2. Methods

The STF is characterized by relatively large horizontal gradients in near-surface temperature and salinity. According to data available at the time, for the most part from the South Atlantic, Deacon (1933, 1937) noted that the surface temperature and salinity changes across the front are often 4°C and 0.5 psu or higher and that surface salinities of at least 34.9 psu obtain in the subtropical waters immediately north of the front. Our observations in the South Atlantic and South Indian oceans (Stramma and Peterson 1990; Stramma 1992) corroborate these identifiers, but as we discuss below, the South Pacific STF is not always so pronounced nor are the near-frontal subtropical waters always quite so salty. Nonetheless, the South Pacific STF is distinguishable, particularly in the distributions of salinity, which are more stable through the seasons than those of temperature.

Our database, extracted from the historical bottle and CTD archives of the World Oceanographic Data Center, current as of June 1993, consists of several quasi-synoptic sections that either cross the front or are in its vicinity. The newest section available to us was made from the RV *Knorr* in September 1978, while the oldest was made from the RV *Carnegie* in December 1928. An additional section made from the RV *Baldrige* in 1990 is also used. These sections for the region between New Zealand and South America are shown in Fig. 1, together with the observed locations of the STF as heavy bars. Table 1 provides a summary of the sections, as well as the surface salinities and temperatures observed at the front. The Tasman Sea is treated separately and is discussed below.

For geostrophic computations in regions where the upper-level flow near the STF is mainly zonal (i.e., away from the western and eastern boundaries), a variable reference is selected at levels where eastward velocities are most likely to be weak or vanishing. According to maps of adjusted steric height by Reid (1986), the axis of the South Pacific subtropical gyre lies between the latitudes of 15° and 25°S at the surface. Beneath this, the axis shifts rapidly southward so that at a depth of 1000–1500 m it lies at roughly 40°S. These levels should have small zonal components of flow in the mean and could be used as reference. However, a more appropriate reference is desired because these levels are still shallow enough that space–time variability could potentially lead to significant zonal velocities, and it is within the upper 1000 m or so that Reid (1986) found most of the vertical shear. At depths of 2000 m and more, the gyre's axis appears to shift back toward the north, but the gradients of adjusted steric height remain weak. At greater depths, a significant change in water masses occurs at about 3000 m near 40°S and 4000 m in the Tropics. A stability maximum exists at this change, above which are low-oxygen, high-silica waters spreading south from the North Pacific and below which are high salinity, low silica waters originating from the North Atlantic that spread north. Most of this meridional motion occurs within deep boundary currents, whereas the broad interior regions at great depth appear to be relatively quiescent. The potential density surface $\sigma_4 = 45.82$ kg m^{-3} (or $\sigma_3 \approx 41.46$ kg m^{-3}) lies near this deep stability maximum and is used as our principal reference for geostrophic calculations. For sections not reaching such depths, we use a reference of $\sigma_2 = 36.75$ kg m^{-3}, which lies at depths of 1500–1900 m, above where the axis

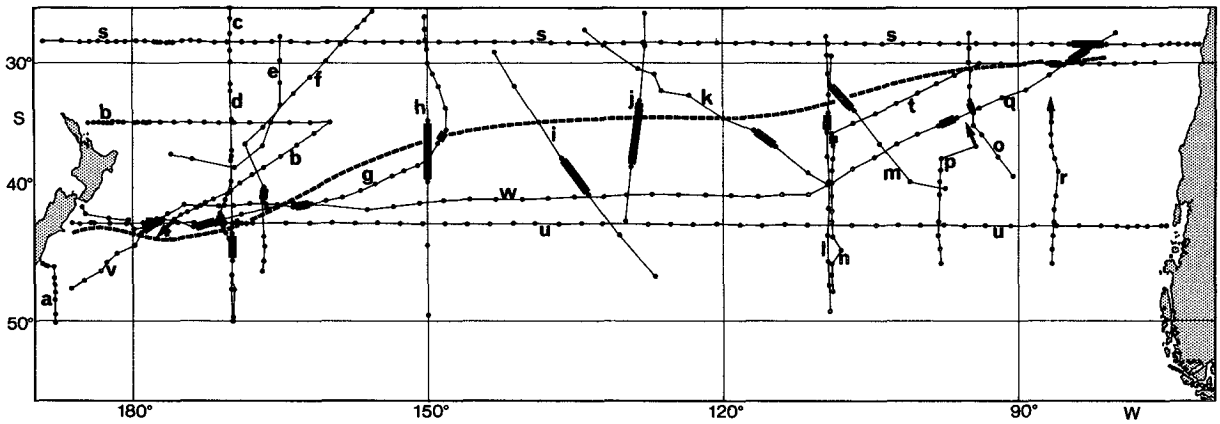

FIG. 1. Sections (lines) and positions (dots) of the hydrographic stations used in the South Pacific. Letters correspond to cruises as listed in Tables 1 and 2. Heavy bars indicate positions of the Subtropical Front, whereas arrows indicate when the front was beyond the denoted ends of the sections. The dashed line indicates the front location according to Deacon (1982). Note that the front was observed at the northwestern end of section (a) but is not demarked because of the close station spacing.

of the subtropical gyre reaches its southernmost extent. It is also below the lower reaches of the Antarctic Intermediate Water (Reid 1973). These choices are consistent with Warren's (1973) generalization of very weak mean flow in the depth range of 1000–3000 m. For stations shallower than these two isopycnal surfaces, we use the deepest common depths between station pairs.

The western boundary of the deep midlatitude South Pacific is represented, north to south, by the Kermadec–Tonga Ridge system and the New Zealand–Campbell Plateau. At depths shallower than 2000 m the western boundary flow is southward along the Kermadec–Tonga Ridge to Chatham Rise (43–44°S), whereas it is northward along the Campbell Plateau (Reid 1986). At depths greater than 2000 m is a con-

TABLE 1. Meridional sections (a)–(r) and zonal sections (s)–(w) appearing in Fig. 1 together with positions of the stations to the immediate south and north (a)–(r) and east and west (s)–(w) of the STF and their surface salinities and temperatures.

Research Vessel	Longitude (deg)	Time	STF location (s: south, n: north)	Surface salinity (psu)	Surface temperature (°C)
(a) *Knorr*	170–172 E	Sep 1978	not s of New Zealand	<34.4	—
(b) *Eltanin*	160–176 W	Sep 1969	s of 42.9°S, 175.9°W	—	—
(c) *Hakuho-Maru*	170 W	Dec 1968	46.0–44.0°S, 170.0°W	34.7–34.9	13.3–15.4
(d) *Baldrige*	170 W	Mar 1990	43.5–42.5°S, 170.6°W	34.6–35.1	15.6–17.8
(e) *Gascoyne*	165–170 W	Jul 1963	s of 39.0°S, 169.7°W	—	—
(f) *Melville*	155–170 W	Mar 1974	41.5–40.5°S, 166.6°W	34.8–35.0	15.4–17.2
(g) *Korolev*	148–160 W	Dec 1970	37.0–35.9°S, 148.5°W	34.6–34.9	16.4–17.3*
(h) *Hudson*	150 W	May 1970	40.0–35.0°S, 150.0°W	34.6–35.3	14.9–18.1
(i) *Hakuho-Maru*	126–143 W	Dec 1971	40.9–38.0°S, 135.0°W	34.2–34.6	13.4–16.2
(j) *Melville*	127–130 W	Apr 1974	38.8–33.5°S, 128.5°W	34.1–34.7	16.5–19.6
(k) *Shoyo Maru*	109–133 W	Nov 1963	37.0–35.8°S, 116.0°W	34.4–34.7	14.6–15.2
(l) *Ob*	109 W	May 1958	35.9–34.2°S, 109.3°W	34.3–34.8	18.6–19.6
(m) *Carnegie*	97–109 W	Dec 1928	34.0–31.8°S, 108.0°W	34.5–34.9	18.9–20.8
(n) *Deryugin*	96–109 W	May 1968	37.0–36.0°S, 109.0°W	34.2–34.5	16.0–17.0
(o) *Shoyo Maru*	90–95 W	Dec 1963	34.3–33.2°S, 94.6°W	34.5–34.7	16.8–17.2
(p) *Deryugin*	94–98 W	May 1968	n of 37.0°S, 94.3°W	—	—
(q) *Deryugin 1*	80–111 W	Jul 1968	35.4–34.7°S, 97.0°W	34.1–34.7	15.0–17.2
(q) *Deryugin 2*	80–111 W	Jul 1968	29.8–28.5°S, 83.1°W	34.5–34.8	17.3–17.8
(r) *Deryugin*	86 W	May 1968	n of 35.0°S, 86.7°W	—	—
(s) *Eltanin*	28 S	Jul 1967	81.0–84.8°W, 28.3°S	34.6–35.0	17.9–18.7
(t) *Deryugin*	30 S	May 1968	85.2–83.2°W, 30.0°S	34.6–34.9	18.5–18.7
(u) *Eltanin*	43 S	Apr 1967	salinity > 34.8 from 179.0°W, 43.2°S to 169.1°W, 43.3°S		
(v) *Korolev*	41–47 S	Dec 1970	salinity 34.8 from 179.2°W, 43.9°S to 161.8°W, 41.8°S		
(w) *Deryugin*	41–44 S	Jul 1968	salinity > 34.8 from 178.9°W, 43.5°S to 171.5°W, 43.0°S		

* Secondary temperature and salinity fronts to the south.

tinuous western boundary current flowing from the south to the north through these domains (Warren 1973; Reid 1986). The region of primary concern here is north of Chatham Rise, so in a manner similar to Warren's (1973) use of a 2000-m reference near the western boundary for two zonal sections made from the RV *Eltanin* at 28° and 43°S, we use the isopycnal $\sigma_2 = 36.75$ kg m^{-3} (about 1800-m depth) as reference for locations west of 170°W. This reference is also used in the Tasman Sea, where the Lord Howe Rise acts as a boundary for flows deeper than 2000 m.

On approaching the eastern boundary, the zonal surface flow bifurcates on the poleward side of 40°S, thus creating an equatorward flow along the coast at more northerly latitudes. The STF is contained within the equatorward branch. However, the near-coastal currents are equatorward in only the upper 200–300 m, beneath which the flow reverses. At 500-m depth, Reid's (1986) map of adjusted steric height indicates poleward near-coastal flow at essentially all latitudes from the equator to the southern tip of the continent, whereas farther offshore the circulation at midlatitudes remains in the same northward direction as in the surface anticyclone. Fortunately, the contrasts in water properties at depth are clear enough to allow for a satisfactory placement of reference levels. As pointed out below, the southward flow along the continental margin can be identified by a salinity maximum lying as shallow as 300 m, directly above which is a minimum carried north from higher latitudes. The transition between these two layers occurs near 250-m depth in our region of interest, so it is there that we place the reference level. Farther offshore, the circulation is northward at depths extending at least through the Antarctic Intermediate Water (Molinelli 1981), so where the southward subsurface flow becomes no longer evident the earlier criteria are used.

3. Observations

a. Tasman Sea

The western South Atlantic and South Indian Oceans have nothing analogous to the Tasman Sea, which is isolated from the deep circulation of the rest of the subtropical South Pacific by a series of islands and ridges. In the upper layers, subtropical waters enter the Tasman Sea from the north along the coast of Australia within the East Australian Current, whose southward transport at 30°–34°S has been estimated as being 35 Sv relative to 1300 db (Andrews et al. 1980). Part of this flow recirculates near the western boundary and another part turns eastward with the Tasman Front, which begins off Australia at 34°–36°S and meanders northeastward to 31°–32°S midway across the Tasman Sea (Mulhearn 1987). The eastward transport at the Tasman Front has been estimated to average near 15 Sv, but larger values can exist in the vicinity of eddies (Andrews et al. 1980). Another destination for the subtropical water is for a small amount to continue moving south along the Australian coast in a progressively more variable current, reaching to as far south as Tasmania (e.g., Wyrtki 1962a) before turning eastward across the southern Tasman Sea in a highly fluctuating pattern. The poleward migration of warm eddies within this regime has been discussed by Nilsson and Cresswell (1981).

In the area near New Zealand, Garner (1959) identified the STF as approximately following the 15°C surface isotherm in summer, the 10°C isotherm in winter, and the 34.7–34.8 isohalines in all seasons. On the basis of a small number of widely spread hydrographic stations, Deacon (1937) observed the STF as extending from south of Tasmania northeastward to the southern end of New Zealand's North Island (near 40°S), while also noting that the front is not as well defined there as it is in the South Atlantic and South Indian Oceans. Wyrtki (1962b) presented a similar picture for the frontal location, also on the basis of scattered data. These descriptions require a termination of the STF on the eastern side of New Zealand. Garner (1959), however, argued that west of New Zealand the front is directed toward the Snares Shelf, which projects poleward from New Zealand, and in his later survey Deacon (1982) depicted the STF as terminating at the southwest corner of South Island before resuming off the northeastern side of the island. Heath (1985a) concurred with the southern orientation of the STF and further described the front as being a continuous feature around the southern end of New Zealand before turning north just east of South Island as the Southland Front and then east along the Chatham Rise near 43°–44°S.

Jeffrey (1986) reviewed all reports of frontal locations in the southern Tasman Sea and concluded that two bands of enhanced surface salinity gradients are usually observed, these at salinities of 34.7 and 35.1 psu. The 34.7 isohaline, which is usually associated with the larger gradient, tends to cross the Tasman Sea zonally from south of Tasmania to south of South Island, whereas the 35.1 isohaline takes a more northerly track from Tasmania toward the southern end of North Island [these paths are also evident in the atlas by Gordon and Molinelli (1982).] Cruise data from the summer of 1988/89 (Warmus 1989; Szymanska and Tomczak 1994) confirm the importance and southern location of the 34.7 isohaline as an indicator for the STF, which tends to support the more recent investigations. It should be noted, however, that extreme variability of the position of the STF in the Tasman Sea is possible. For example, if the STF is a result of Ekman pumping, the variability in curl of wind stress should give some indication of the variability of the STF position. Streten (1980) analyzed the Southern Hemisphere atmospheric circulation and found the largest seasonal and interannual variability in the Tasman Sea and western South Pacific Ocean. The various

reported STF locations could therefore be a result of atmospheric conditions. Variability of the large-scale oceanic circulation could also play a role; Szymanska (1994, personal communication) reports that in an ocean circulation model of the Southern Hemisphere the position of the STF in the eastern Tasman Sea can be anywhere between the southern end of South Island and the northern end of North Island, depending on the amount of flow allowed to pass through the Indonesian Seas.

Deep hydrographic sections in the WODC dataset are surprisingly few in number for the Tasman Sea (Fig. 2a). As described above, we compute geostrophic transports in the upper 1000 m in this region by using the isopycnal surface $\sigma_2 = 36.75$ kg m^{-3} (depth about 1800 m) as reference. Nonsynopticity of the data leads to mass imbalances calculated within the area enclosed by the sections, which should be expected because of the vigorous eddy field but which probably does not seriously affect the validity of the observed patterns. The southward transport of the East Australian Current is found to be 38 Sv at 34°S (Fig. 2b), 22 Sv of which recirculate while 14 Sv meander eastward near 33°S at the Tasman Front and 2 Sv leave to the north at 158°E. These figures are similar to those by Andrews et al. (1980). Nine Sverdrups of the latter are provided to the East Auckland Current. The 34.7 and 35.1 isohalines at the surface are shown in Fig. 2a. The 34.7 isohaline corresponds well in position with previous reports of a southern location of the STF, except that the isohaline turns to the north just west of South Island. Away from a recirculating cell near Tasmania, there is a general, but weak, eastward flow in the vicinity of the STF. It is only about 3 Sv, and it does not leave the Tasman Sea. The weakness of flow associated with the STF here is likely a result of the southward extent of New Zealand, which prohibits any significant amount of subtropical water from flowing around to the south; the Tasman Sea would thus seem to be a subtropical water cul de sac characterized by mixing. South of STF and north of 50°S the velocities are small and are directed mainly to the west. South of 50°S two eastward jets within the Antarctic Circumpolar Current are found, but those transports are peripheral to this work and would have to be calculated with a deeper reference.

In the area between the STF and the Tasman Front the computed velocities are variable in direction and do not point toward an organized flow. The pair of short shallow sections south of New Zealand indicate weak flows with maximum eastward transport of 0.5 Sv. The present data distribution is too small for detailed investigation of the southern Tasman Sea, but the data are useful in the sense that they show the flow at the STF in the Tasman Sea as being weak and that most of the water in the East Australian Current either recirculates or flows along the Tasman Front to contribute to the East Auckland Current.

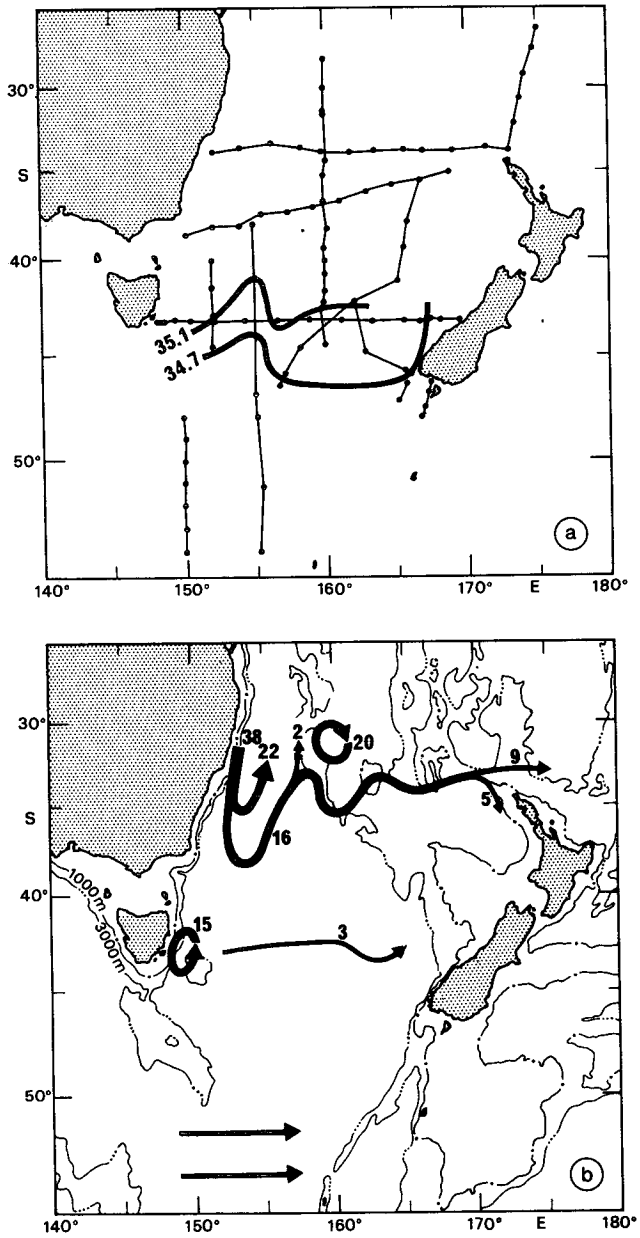

FIG. 2. (a) Sections (thin lines) and positions (dots) of the hydrographic stations used in the Tasman Sea. Heavy lines denote the indicated surface isohalines. (b) Schematic representation of the geostrophic flow field together with volume transports (excluding the Antarctic Circumpolar Current) in the upper 1000 m relative to the isopycnal surface $\sigma_2 = 36.75$ kg m^{-3} (depth about 1800 m). Major bottom relief is illustrated with selected isobaths at 1000 (line with one dot) and 3000 m (line with three dots).

b. *Open South Pacific*

The continuation of the STF east of New Zealand appears to be independent of its location in the Tasman Sea. East of Chatham Rise, Heath (1981) found the STF to loop southward as a tonguelike feature, while more recently Butler et al. (1992) used a set of satellite

infrared images and in situ data to find that the subtropical water moving around the southern end of South Island is confined to only a narrow ribbon along the coast. This seems to be consistent with a late winter section made off South Island by the RV *Knorr* in 1978 (section a in Fig. 1). In this, only the most inshore station was made in subtropical water (11°C and 34.9), but because it was made to just 100-m depth we do not make geostrophic calculations. These data were taken as part of a larger survey off South Island, and in the remainder of the survey only a small detached eddy with subtropical characteristics was sampled. This eddy was centered near 46°S, 175°E, probably deriving from a southward meander of the STF east of New Zealand, though it could have also originated west of New Zealand before taking an eastward path around the southern end of the island. Heath (1985b) has also observed warm eddies in the region.

Eastward from New Zealand, the STF is well discerned, though less so than in the South Atlantic and South Indian Oceans. It is found near 44°S in the vicinity of the date line and from there it gradually shifts northward downstream. In Fig. 1 the STF locations are given as heavy bars, while the front location presented by Deacon (1982) is shown as a dashed line. Deacon (1982) used all available data from the National Oceanographic Data Center archives of 1974 to map the surface position of the 34.9 isohaline around the hemisphere, which he associated with the STF. The differences between our locations, based on quasi-synoptic sections, and Deacon's (1982) locations which were based on all data, arise at least in part from the use of somewhat different criteria, and they may also reflect the degree to which the STF can migrate meridionally, perhaps up to 2–3° latitude. Belkin et al. (1988) also investigated the STF in the South Pacific and described a broader subtropical frontal zone, the northern side of which intersects 90°W at approximately 33°S before curving more strongly north as the South American boundary is approached, and our representation is similar to this.

For synoptic station pairs defining the STF (from Table 1), the average differences in temperature and salinity from one side of the front to the other are only 1.5°C and 0.4, whereas in the Atlantic they are 2.2°C and 0.6 (Stramma and Peterson 1990), and 3.7°C and 0.7 in the Indian Ocean (Stramma 1992). Although these numbers have no real quantitative meaning, as they come from stations made at different locations relative to the front and by station pairs having different horizontal separations, the qualitative aspect of the South Pacific STF being less pronounced is probably valid. This is also reflected by the South Pacific Current having relatively weak eastward geostrophic velocities and transports (Table 2). The largest surface velocity observed for the current is just under 10 cm s^{-1} (section 1, made by the RV *Ob*). But as can be seen in Fig. 1, the sections in the middle portions of the basin have very large station spacings, particularly at sections h and j where they approach 500 km, which will naturally lead to underestimations of maximum velocities and possibly aliased transports due to eddies. The historical database presently available for the South Pacific has little more to offer, but a closely spaced meridional section (0.5° station spacing) along 135°W has recently been made from the RV *Knorr* in 1992. Preliminary data (J. Reid 1994, personal communication) show that the STF was located at 35°–36°S with surface temperatures and salinities of 15–17°C and 34.5–35.0. The maximum eastward geostrophic speed, relative to 3500-m depth, was about 11 cm s^{-1} at the front, diminishing to near zero at 500 m. It carried no more than 5 Sv.

Examples of late-summer thermohaline and velocity fields in the western South Pacific, made from the RV *Baldrige* along 170°W (section d in Fig. 1), are shown in Fig. 3. The station spacing was adequate for satisfactory resolution of the STF, which was crossed directly over Chatham Rise in a manner similar to that which has been reported by Heath (1985a). There was also a small lens of relatively salty water south of the front in this *Baldridge* section. As compared with the western portions of the South Atlantic and South Indian Oceans, the STF here had conspicuously weak signatures in the thermohaline fields, but nonetheless the horizontal temperature gradients are noticeable to a depth of 1500 m and those in salinity to 800 m. Associated with these gradients was a band, less than 200 km wide, of enhanced eastward velocities. The maximum speed, 7 cm s^{-1}, was attained at the surface, and there were speeds of 4 cm s^{-1} at depths of nearly 500 m. The total transport for the current in the upper 1000 m was less than 5 Sv, or just 20% of the transport typical for the STF in the western South Atlantic (Stramma and Peterson 1990). Velocities poleward of the STF remained less than ~2 cm s^{-1} until the salinity minimum of the Antarctic Intermediate Water began its rapid rise into the northern Antarctic Circumpolar Current, which normally continues until the minimum reaches the surface on the southern side of the Subantarctic Front. The axis of the South Pacific Current was more than 500 km north of where the zonal velocities began to increase in the northern Antarctic Circumpolar Current. The velocities shown there in Fig. 3c, just over 10 cm s^{-1}, are underestimates because a more realistic reference would be at the bottom, and because we terminate the sections in the northern reaches of the current. Also, another region of enhanced eastward flow in this section is observed north of the South Pacific Current, near 30°S, which corresponds to an eastward extension of the East Australian Current around the northern end of New Zealand (Fig. 1 in Wyrtki 1962a). Tsuchiya (1982) also made note of this feature, while in the dynamic topography map by Heath (1985a) there is a splitting of the East Auckland Current north of New Zealand into an eastward flow

TABLE 2. Depths of the potential density surface of σ_4 = 45.82 kg m^{-3} (marked by @) or σ_2 = 36.75 kg m^{-3} used as reference for geostrophic calculations, together with maximum eastward geostrophic speeds at the surface for the South Pacific Current (SPC) and eastward geostrophic transports (1 Sv = 10^6 m^3 s^{-1}) in the upper 1000 m for the station pairs spanning the Subtropical Front (STF, shown as heavy bars in Fig. 1). Transport values for regions north of the STF are computed from the front northward to either the end of the particular section or until reversal in flow direction is encountered. The final column gives transport values for station pairs immediately south of the STF. For zonal sections positive values are northward. In the northeast reference and transport are to 250-m depth only.

Research Vessel	Longitude	Reference depth (m)	Maximum velocity (cm s^{-1}) of SPC	Transports (Sv)		
				At STF	North of STF	South of STF
(a) *Knorr*	170°–172°E	420#–1280#	NA	NA	NA	NA
(b) *Eltanin*	160°–176°W	840#–1720	NA	NA	5.2	NA
(c) *Hakuho-Maru*	170°W	1810–1860	1.3	−0.1	−1.0	−2.3
(d) *Baldrige*	170°W	1800–1840	7.0	3.2	0.8	−0.4
(e) *Gascoyne*	165°–170°W	1590#–1790	NA	NA	NA	NA
(f) *Melville*	155°–170°W	1730–1770	3.5	1.6	6.5	2.4
(g) *Korolev*	148°–160°W	610#–1560#	3.5	−1.9	2.1	1.6
(h) *Hudson*	150°W	3030–3230@	1.6	−2.2+	−4.3+	1.8+
(i) *Hakuho-Maru*	126°–143°W	3100–3150@	3.8	6.2	−3.8	0.1
(j) *Melville*	127°–130°W	2560#–3210@	0.7	−5.4+	−2.1+	0.3+
(k) *Shoyo Maru*	109°–133°W	450#–650#	3.2	1.8	2.4	0.6
(l) *Ob*	109°W	1160–1620	9.9	−2.3	6.1	−5.3
(m) *Carnegie*	97°–109°W	1580–1660	5.3	5.5	4.3	1.0
(n) *Deryugin*	96°–109°W	1100#–1230#	5.1	2.1	0.8	−0.7
(o) *Shoyo-Maru*	90°–95°W	560#–580#	5.7	1.6	3.4	1.0
(p) *Deryugin*	94°–98°W	1110#–1190#	NA	NA	NA	NA
(q) *Deryugin 1.*	80°–111°W	780#–1510#	4.3*	0.2*	2.5*	−5.0*
(q) *Deryugin 2.*	80°–111°W	250	−2.2*	−1.1*	−0.1*	−0.1*
(r) *Deryugin*	86°W	770#–1170#	NA	NA	NA	NA
	Latitude			At STF	East of STF	West of STF
(s) *Eltanin*	28°S	250	1.5	0.5	0.7	0.0
(t) *Deryugin*	30°S	250	1.5	0.3	1.8	−0.2
(u) *Eltanin*	43°S	1720–1740	3.6	2.4	−0.8	−0.5
(v) *Korolev*	41°–47°S	320#–1720#	5.1	1.9	2.8	2.4
(w) *Deryugin*	41°–44°S	too shallow	NC	NC	NC	NC

@ Reference depth σ_4 = 45.82 kg m^{-3}.
# Deepest depth available.
* Positive to the southeast, NA: not available, NC: not computed.
+ Station spacing too large to estimate transport.

near 30°S and a southward flow known as the East Cape Current into the region where the South Pacific Current is formed. This splitting is not evident in our data, which might be due to differences in reference depths.

For the central South Pacific, the thermohaline and velocity fields made from the RV *Hakuho-Maru* at 126°–143°W in summer (section i in Fig. 1) are shown in Fig. 4. The station spacing in the vicinity of the STF was about 300 km, so the front was not well resolved. It was crossed somewhere between 38° and 40.9°S, and as in the RV *Baldrige* section, the surface temperature and salinity changes were less than 3°C and 0.5. These surface gradients were associated with an eastward current that carried, according to this coarse resolution, about 6 Sv in the upper 1000 m and which was flanked on each side by broad regions of weak flow. As with the RV *Baldrige* section at 170°W, the temperature and salinity gradients as well as the velocity signatures were restricted to the upper ocean. Also as with the 170°W RV *Baldrige* section, an eastward current band existed near 30°S, which had higher surface velocities than that near 40°S.

The southeastern corner of the subtropical gyre was crossed by a diagonal winter section made from the RV *Deryugin* (Fig. 5; section q in Fig. 1), so the STF was intersected twice. The front had shifted north to about 35°S at 97°W, where it remained relatively clear, especially in the salinity field, but the horizontal gradients and geostrophic flow associated with the front extended to only about 200–300-m depth. Here the South Pacific Current carried about 3 Sv before the STF turned north. Immediately southwest of the front was an anticyclonic eddy that reached to about 800-m depth, but the upper-level salinities of near 34.1 were not of subtropical origin. They were likely the product of the low salt tongue that extends westward from the South American coast, discussed below.

With downstream warming and modification of the adjacent subantarctic waters as the front turned north, the STF became noticeably more diffuse. At the frontal intersection, near 29°S 83°W, were surface tempera-

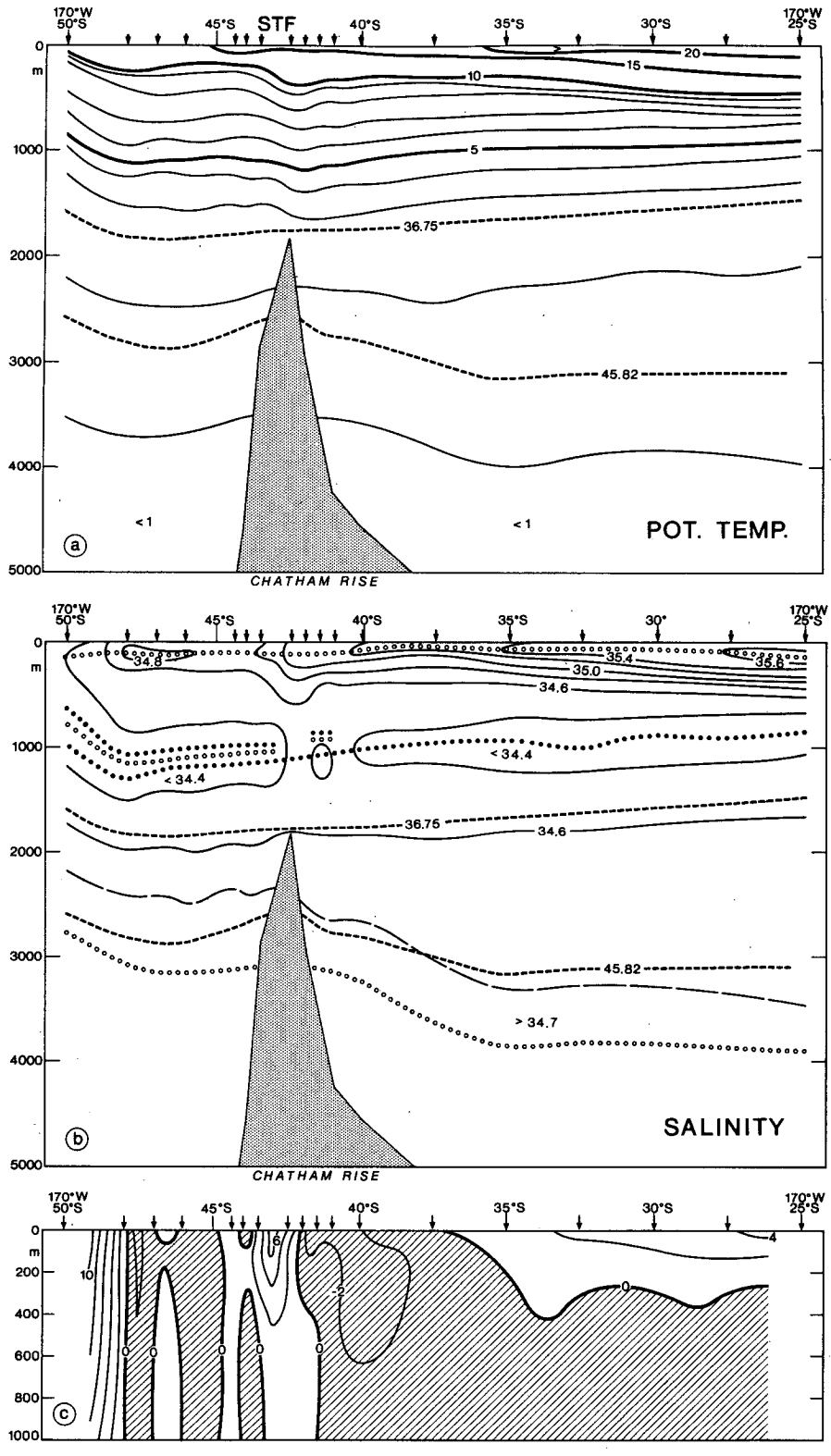

FIG. 3. Vertical distributions of (a) potential temperature (°C), (b) salinity, and (c) eastward geostrophic speed (cm s^{-1}) in the upper 1000 m (westward speed is shaded) relative to the potential density surface σ_2 = 36.75 kg m^{-3} along the south (left) to north (right) line of stations (arrows) occupied by RV *Baldrige* at 170°W in March 1990 (section d). Relative maxima are denoted by open circles, and minima by dots. Also shown with broken lines are the isopycnals σ_2 = 36.75 kg m^{-3} and σ_4 = 45.82 kg m^{-3}. STF indicates the STF location.

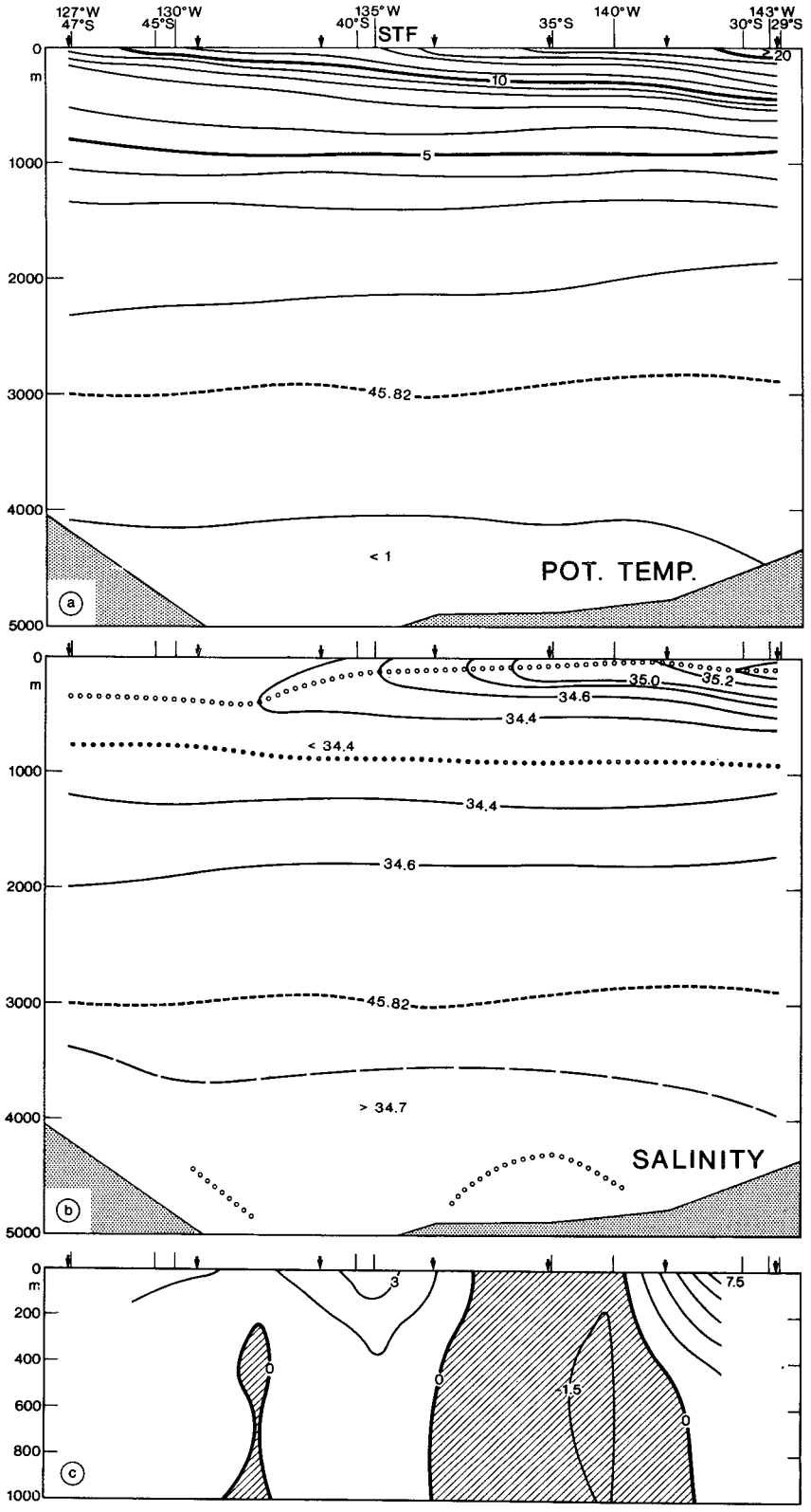

FIG. 4. Vertical distributions of (a) potential temperature (°C), (b) salinity, and (c) northeastward geostrophic speed (cm s^{-1}) in the upper 1000 m (southwestward speed is shaded) relative to the potential density surface σ_4 = 45.82 kg m^{-3} along the southeast (left) to northwest (right) line of stations (arrows) occupied by RV *Hakuho-Maru* at 126°–143°W in December 1971 (section i). Relative maxima are denoted by open circles and minima by dots. Also shown with the broken line is the isopycnal σ_4 = 45.82 kg m^{-3}. STF indicates the STF location.

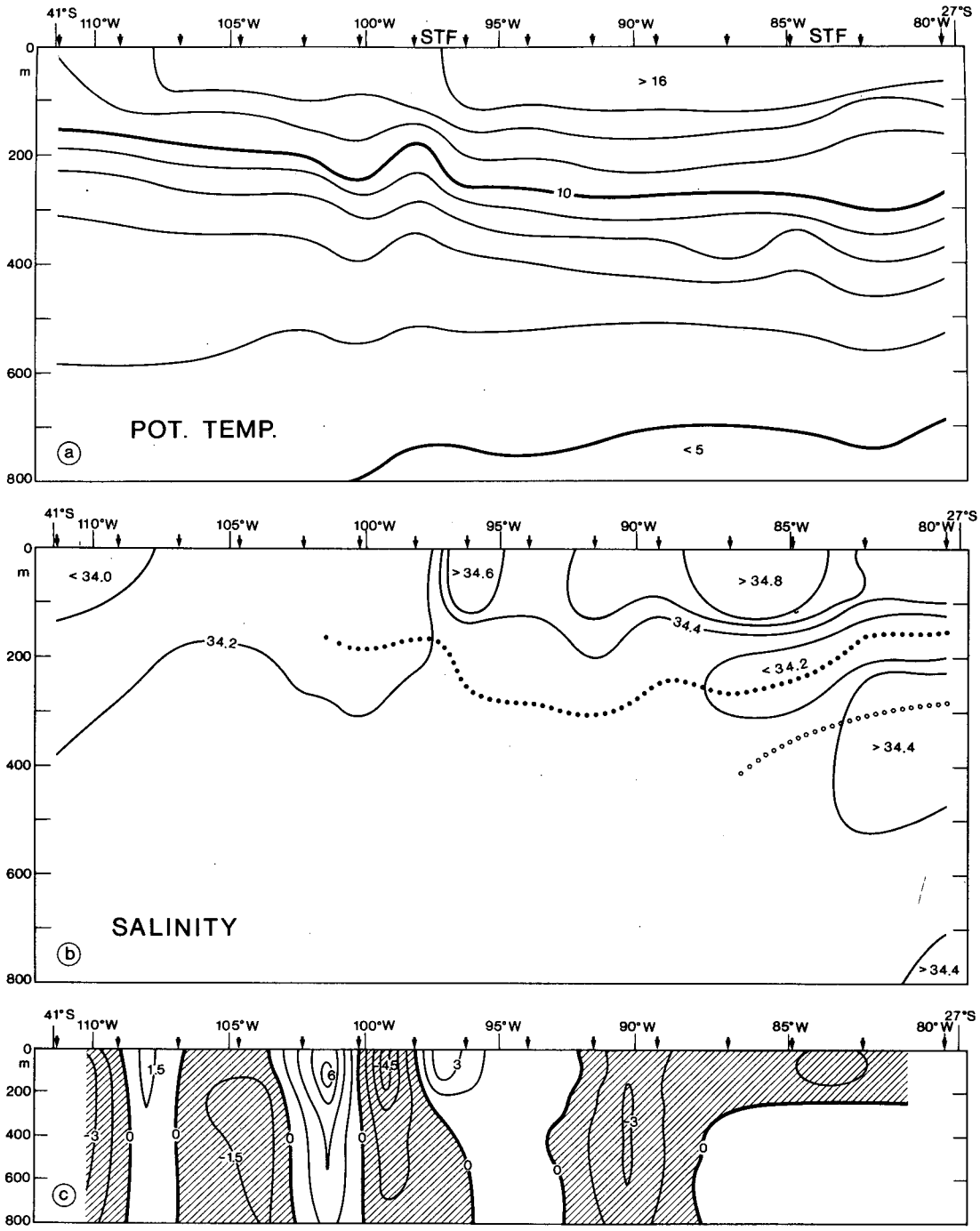

FIG. 5. Vertical distributions in the upper 800 m of (a) potential temperature (°C), (b) salinity, and (c) southeastward geostrophic speed (cm s^{-1}) (northwestward speed is shaded) along the southwest (left) to northeast (right) line of stations (arrows) occupied by RV *Deryugin* at 80°–111°W in July 1968 (section q). The reference level begins in the southwest on the potential density surface $\sigma_2 = 36.75$ kg m^{-3} and rises to approximately 250 m near the South American coast. Relative maxima are denoted by open circles, and minima by dots. STF indicates the STF location.

ture and salinity changes of just 0.5°C and 0.3. By using the greatest depths available (780–1510 m) for making geostrophic computations, a total northwestward transport for the current band of 9 Sv is obtained, and this is artificially large. Unlike the previous regions where such a reference is acceptable, the flow normal to this section near the eastern boundary has a reversal with depth that must be taken into consideration. A

salinity minimum occurs near the eastern boundary at depths of 150–250 m (Fig. 5b), which identifies a layer moving north from subantarctic origins with the surface circulation, whereas an underlying salinity maximum was measured that signals a poleward countercurrent that appears to extend to the bottom (Reid 1986). By using a more reasonable reference level between the salinity minimum and underlying maximum, the northward extension of the South Pacific Current is observed to carry only about 1.3 Sv. A pair of winter zonal sections made by the RV *Eltanin* and the RV *Deryugin* along 28° and 30°S (sections s and t in Fig. 1 and Table 1) crossed the STF at comparable longitudes, and the frontal signatures and associated flow were similarly weak.

c. *Antarctic Intermediate Water*

It has been proposed that the Antarctic Intermediate Water (AAIW) derives from subantarctic mode water (SAMW), produced by deep (400–600 m) vertical convection in late winter of upper waters in the southern Subantarctic Zone of the Antarctic Circumpolar Current, instead of from the northward spreading, mixing, and subduction of surface waters from the Antarctic and Polar Frontal zones farther south (McCartney 1977). In particular, the densest varieties of SAMW (σ_0 = 27.10 kg m^{-3}) were found in the southeast Pacific Ocean and Scotia Sea, and these were seen as being identical with the AAIW in the southern South Pacific and South Atlantic with respect to temperature and salinity (see also McCartney 1982). The Subantarctic Zone lies immediately south of the STF, and although that zone extends farther south than most of our sections, it seems worthwhile to take a look at manifestations of vertical mixing in our data in relation to the AAIW layer.

The data we are using come primarily from the southern summer and fall, and except for a short section south of New Zealand (a in Fig. 1), none south of the STF come from late winter, so we cannot expect to see any direct evidence of convective overturning. But there is a layer beneath the seasonal thermocline that has a pronounced lack of vertical stratification. Shown in Figs. 6 a–c are vertical sections of potential vorticity (fE, where f is the Coriolis parameter and E is static stability) plotted against potential density as ordinate along lines from the western, central, and eastern portions of the basin. The weakest stratification occurs at σ_0 = 26.9–27.1 kg m^{-3} (roughly the depth range 500–800 m) in each section, with the lowest values appearing at and south of the STF. North of the STF, especially in the east, the stratification increases while the minimal values descend to greater densities, thus indicating an accelerated erosion of the layer from above once it spreads beneath subtropical waters.

Whether the minima in potential vorticity in the upper reaches of the AAIW are produced from winter convection in the surface layer of the Subantarctic Zone or whether they are a result of northward spreading, mixing, and sinking of surface waters from farther south is indeterminable. But what appears to be true is that the most vertically homogeneous layer, just above the core of the AAIW south of the STF, is inhibited from direct northward spreading by the enhanced eastward flow of the South Pacific Current.

4. Discussion

The goal of this work has been to investigate the geostrophic flow associated with the South Pacific Subtropical Front. Clearly, the historical database available for doing so is marginal, as two of the sections in the middle of the basin (h and j in Tables 1 and 2) have station spacings approaching 500 km in the vicinity of the STF, thus rendering the velocity computations from them invalid for inferring flow patterns associated with the front. But a new meridional section made during the World Ocean Circulation Experiment in the middle part of the basin confirms the transport estimates. In the southern Tasman Sea a weak eastward flow of 3 Sv is observed at the STF, but most of this probably recirculates back toward the north within the Tasman Sea before exiting north of New Zealand. Off the eastern coast of New Zealand the South Pacific Current begins as a combination of a narrow band of subtropical water flowing around the southern end of South Island and a larger component of subtropical water apparently supplied from an eastward extension of the East Australian Current flowing to the east along the Tasman Front and then around the northern end of North Island as the East Auckland Current (Roemmich and Cornuelle 1990) and then southward as East Cape Current (e.g., McCartney 1982).

In the zonal section we have used that crossed the East Auckland Current, all of its 10-Sv transport returned north to contribute 6 Sv to the current band near 30°S. In other observations (Heath 1985a), however, a contribution from the East Auckland Current to the South Pacific Current can be seen. In our data we find the South Pacific Current well defined just east of New Zealand over Chatham Rise, from where it shifts generally northward to 30°–35°S as it nears South America, and finally it turns more strongly north offshore of the equatorward-moving subantarctic water (Fig. 7). The STF bounds the outer edge of the current as it turns north and does not separate from the current near the eastern boundary as it does in the South Atlantic and South Indian Oceans. Although the database in the central portions of the South Pacific is scant, it is likely that the South Pacific Current is continuous across the basin and that it forms the southern closure to the subtropical gyre circulation well north of the zonal jets of the Antarctic Circumpolar Current.

Hofmann (1985) used undrogued surface buoys to investigate the structure of the Antarctic Circumpolar

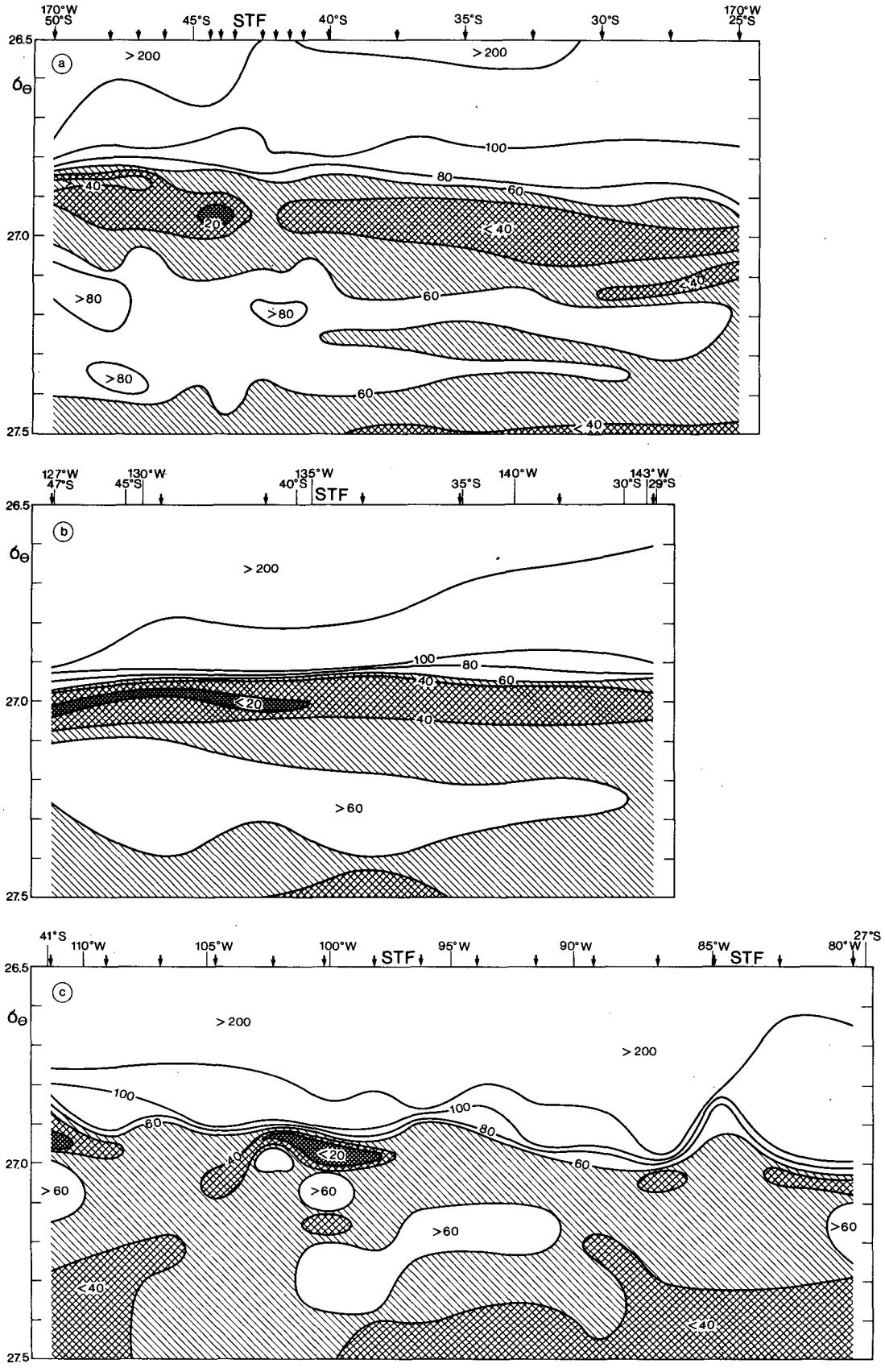
170°W
50°S
45°S
STF
40°S
35°S
30°S
170°W
25°S
26.5
a
> 200
> 200
σθ
100
80
60
40
20
< 40
< 40
> 80
> 80
60
> 80
60
27.0
27.5
< 40
127°W
47°S
130°W
45°S
135°W
40°S
STF
35°S
140°W
143°W
30°S
29°S
b
> 200
100
80
40
60
20
40
> 60
41°S
110°W
105°W
100°W
STF
95°W
90°W
85°W
STF
80°W
27°S
c
> 200
> 200
100
100
60
80
40
20
60
> 60
> 60
> 60
> 60
< 40
< 40

Current. The buoy track distribution (her Fig. 2) reflects similar features in the South Pacific circulation as the flow field described here. East of New Zealand the region with the largest number of buoy trajectories is located south of 40°S and moves north of 40°S at about 145°W. Also, the turn of the East Australian Current into an eastward flow along the Tasman Front passing just north of New Zealand and continuing to the east near 30°S can be seen in the buoy track distribution. The largest difference with our transport field is a large concentration of buoys west and south of the southern tip of New Zealand with there being an impression of northward flow along each side of South Island. This is likely caused by the buoys following the shallow Ekman layer over shallow topography where the geostrophic transport is actually quite small.

A pair of somewhat surprising results are that the South Pacific Current starts out east of New Zealand by transporting only around 5 Sv in the upper 1000 m and that it remains near this strength across most of the basin before it becomes shallower and weaker near the eastern boundary. This is in sharp contrast with the currents associated with the STF in the other two basins, where they transport 30 Sv or more in the western portions before weakening to 10–15 Sv in the eastern portions.

The relative weakness of the South Pacific Current might have been anticipated from earlier studies, though, such as that by Reid and Arthur (1975) whose map of geopotential anomaly at the sea surface implies that flow in the region of the STF is weaker than flows to its north and south. Also, analyses of ship drifts (Wyrtki et al. 1976) and drifting buoy trajectories (Patterson 1985) show mean energies in the midlatitude South Pacific that are considerably lower than in the corresponding portions of the other basins. From the transport fields it can be seen that there are two eastward current bands in the South Pacific. The larger part of the East Australian Current flows along the Tasman Front and continues east of New Zealand as a northern current band near 30°S, while a smaller amount of subtropical water flows in the southern current band at the STF. The northern current band is well represented in the potential vorticity distribution in Keffer's (1985, his Fig. 5) map for the layer σ_0 = 26.05–26.25 kg m^{-3}.

Reasons why the South Pacific Current should be so much weaker than its Southern Hemisphere counterparts are not particularly clear, but it would seem that at least three mechanisms are involved. One is the presence of New Zealand and the bathymetric structures to its north that have no equivalents in the other basins. Unlike the southern extremities of the Brazil and Agulhas Current systems, where southward flow extends to great depth, much of the upper-level flow in the western South Pacific is decoupled from the deeper flow when the East Australian Current is fed by waters passing over shallow bathymetry. The upper-level western boundary currents off New Zealand thus provide the South Pacific Current with relatively little to start with.

Another mechanism is the vertical structure of circulation in the middle of the South Pacific that is also quite different from what exists in the South Atlantic and South Indian Oceans. In the South Pacific, the axis of the subtropical gyre shifts farther south with increasing depth than do those in the other basins. In the South Atlantic there is a nearly continuous eastward flow along 40°S from the surface down to almost 3000 m (according to adjusted steric height fields given by Reid 1989), and the same appears to hold true in the Indian Ocean for regions west of Australia (Wyrtki 1971); the axes of these two gyres remain north of the surface STF. By contrast, Reid (1986) has shown the axis of the South Pacific subtropical gyre to shift to about 40°S in the depth range 1000–1500 m, in which case there is essentially no zonal flow at these depths. If there were instead an important eastward component there, an increment in velocity of each centimeter per second at 1000 m, applied to a current width of 100 km, would lead to an increase in transport of 1 Sv. But even with an increase in eastward speed of 10 cm s^{-1} at 1000 m, the transport of the current would increase to just 15 Sv, which would still be significantly lower in the western part of the basin than in the western South Atlantic and South Indian Oceans, so this alone does not account for why the upper-level vertical shears and volume transports in this domain of the South Pacific should be so small.

A third mechanism might be strong poleward eddy heat and salt fluxes in the upper levels from the subtropics to the Southern Ocean in the Atlantic and Indian sectors. Being that the subtropical gyres are closed well north of the Antarctic Circumpolar Current and that upper-level heat and salt transport into the Southern Ocean cannot be accomplished directly by the subtropical western boundary currents, there must be large property transports across the STF, presumably by the eddy field near the western boundaries. We find eddies of subtropical water south of the STF in the western South Pacific, but these are small compared with those typically found in the western South Atlantic and those shed from the Agulhas Current Retroflection. Indeed, all maps of variability at the sea surface (e.g., Cheney

FIG. 6. Potential vorticity (fE in 10^{-14} cm^{-1} s^{-1}) with potential density as section ordinate for (a) RV *Baldrige* at 170°W in March 1990 (section d, Fig. 3), (b) RV *Hakuho-Maru* at 126°–143°W in December 1971 (section i, Fig. 4), and (c) RV *Deryugin* at 80°–111°W in July 1968 (section q, Fig. 5). STF indicates the STF location.

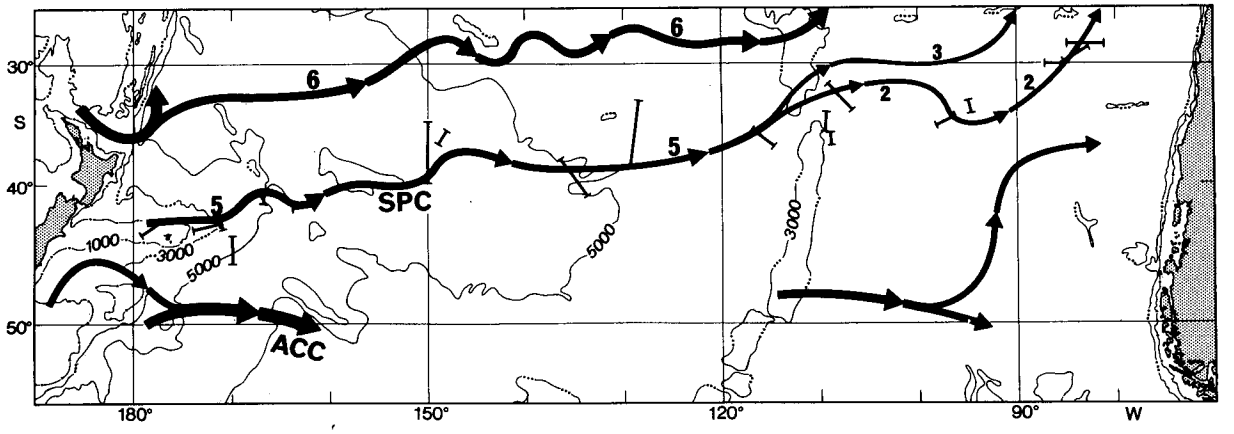

FIG. 7. Schematic depiction of the South Pacific Current (SPC), with volume transports given for the upper 1000 m in Sverdrups. The bars show the STF location as shown in FIG. 1. Also shown is an eastward band lying several degrees north of the SPC, as well as the position of the northern branch of the Antarctic Circumpolar Current, the Subantarctic Front, where it appeared in our sections but without transport values because of inadequate resolution. The main bathymetric features are illustrated with selected isobaths at 1000 (line with one dot), 3000 (line with three dots), and 5000 m (solid line).

et al. 1983; Patterson 1985; Chelton et al. 1990) show the western South Pacific off New Zealand as having a great deal less mesoscale energy than do the western portions of the other basins. These maps, however, do reveal large eddy energies in the East Australian Current, but this variability appears to extend only to the northernmost part of Tasmania and, unlike in the other basins, not to latitudes of the STF. Heath (1985b) proposed that the variability in the East Australian Current results primarily from baroclinic instabilities arising from intense vertical shears in a shallow current, so it is probable that the eddy field there has little impact on heat and salt fluxes into the Southern Ocean. By contrast, there can be little doubt about the importance of eddy heat and salt fluxes into the northern Antarctic Circumpolar Current in the Atlantic and Indian sectors, and these might have the cumulative downstream effect of causing the northern Antarctic Circumpolar Current entering the Pacific sector to be anomalously warm and salty. Hemispheric charts in the atlas by Gordon and Molinelli (1982) indicate that such is the case. The relative weakness of the South Pacific Current thus appears due to a combination of effects arising from geomorphology, vertical structure of the South Pacific subtropical gyre, and eddy heat and salt fluxes into the northern Antarctic Circumpolar Current in the other two basins.

Acknowledgments. This study has been supported by grants from the Deutsche Forschungsgemeinschaft (LS), the National Science Foundation (RGP, OCE-9116191), and the Australian Research Council (MT). We are indebted to the late Stan Hayes for kindly providing the RV *Baldrige* data along 170°W (cruise MB-90-02). We thank Lynne Talley and Joe Reid for the very preliminary information from the RV *Knorr* section along 135°W, and A. Eisele for drafting the figures.

REFERENCES

Andrews, J. C., M. V. Lawrence, and C. S. Nilsson, 1980: Observations of the Tasman Front. *J. Phys. Oceanogr.*, **10,** 1854–1869.

Belkin, I. M., Yu. M. Gusev, and L. A. Levin, 1988: The surface thermohaline fronts of the South Pacific (in Russian). *Ecosystems of the subantarctic zone of the Pacific Ocean.* M. E. Vinogradov and M. V. Flint, Eds., Nauka, 303.

Butler, E. C. V., J. A. Butt, E. J. Lindstrom, P. C. Tildesley, S. Pickmere, and W. F. Vincent, 1992: Oceanography of the subtropical convergence zone around southern New Zealand. *New Zealand J. Mar. Freshwater Res.*, **26,** 131–154.

Chelton, D. B., M. G. Schlax, D. L. Witter, and J. G. Richman, 1990: GEOSAT altimeter observations of the surface circulation of the Southern Ocean. *J. Geophys. Res.*, **95,** 17 877–17 903.

Cheney, R. E., J. G. Marsh, and B. D. Beckley, 1983: Global mesoscale variability from collinear tracks of SEASAT altimeter data. *J. Geophys. Res.*, **88,** 4343–4354.

Deacon, G. E. R., 1933: A general account of the hydrology of the South Atlantic Ocean. *Discovery Rep.*, **7,** 171–238.

——, 1937: The hydrology of the Southern Ocean. *Discovery Rep.*, **15,** 3–122.

——, 1982: Physical and biological zonation in the Southern Ocean. *Deep-Sea Res.*, **29,** 1–15.

Garner, D. M., 1959: The subtropical convergence in New Zealand surface waters. *New Zealand J Geol. Geophys.*, **2,** 315–337.

Gordon, A. L., and E. J. Molinelli, 1982: *Southern Ocean Atlas: Thermohaline and Chemical Distributions.* Columbia University Press, 11 pp and 233 plates.

Heath, R. A., 1981: Oceanic fronts around southern New Zealand. *Deep-Sea Res.*, **28,** 547–560.

——, 1985a: A review of the physical oceanography of the seas around New Zealand. *New Zealand J. Mar. Freshwater Res.*, **19,** 79–124.

——, 1985b: Large scale influence of the New Zealand seafloor topography on the South Pacific Ocean western boundary currents. *Aust. J. Mar. Freshwater Res.*, **36,** 1–14.

Hofmann, E. E., 1985: The large-scale horizontal structure of the Antarctic Circumpolar Current from FGGE drifters. *J. Geophys. Res.*, **90,** 7087–7097.

Jeffrey, M. Z., 1986: Climatological features of the Subtropical Convergence in Australian and New Zealand waters. University of Sydney Ocean Sciences Institute Report 17, 96 pp.

Keffer, T., 1985: The ventilation of the world's oceans: Maps of the potential vorticity field. *J. Phys. Oceanogr.*, **15,** 509–523.

McCartney, M. S., 1977: Subantarctic Mode Waters. *Deep-Sea Res.*, **24,** (Suppl.), 103–119.

——, 1982: The subtropical recirculation of Mode Waters. *J. Mar. Res.*, **40,** (Suppl.), 427–464.

Molinelli, E. J., 1981: The Antarctic influence on Antarctic intermediate water. *J. Mar. Res.*, **39,** 267–293.

Mulhearn, P. J., 1987: The Tasman Front: A study using satellite infrared imagery. *J. Phys. Oceanogr.*, **17,** 1148–1155.

Nilsson, C. S., and G. R. Cresswell, 1981: The formation and evolution of East Australian Current warm-core eddies. *Progress in Oceanography,* Vol. 9, Pergamon, 133–183.

Patterson, S. L., 1985: Surface circulation and kinetic energy distributions in the Southern Hemisphere oceans from FGGE drifting buoys. *J. Phys. Oceanogr.*, **15,** 865–884.

Reid, J. L., 1973: Transpacific hydrographic sections at lats. 43°S and 28°S: The SCORPIO-Expedition. III: Upper water and a note on southward flow at mid-depth. *Deep-Sea Res.*, **20,** 39–49.

——, 1986: On the total geostrophic circulation of the South Pacific Ocean. Flow pattern, tracers and transports. *Progr. Oceanogr.*, **16,** 1–61.

——, 1989: On the total geostrophic circulation of the South Atlantic Ocean: Flow pattern, tracers and transports. *Progr. Oceanogr.*, **23,** 149–266.

——, and R. S. Arthur, 1975: Interpretation of maps of geopotential anomaly for the deep Pacific Ocean. *J. Mar. Res.*, **33,** (Suppl.), 37–52.

Roemmich, D., and B. Cornuelle, 1990: Observing the fluctuations of gyre-scale ocean circulation: A study of the subtropical South Pacific. *J. Phys. Oceanogr.*, **20,** 1919–1934.

Stramma, L., 1992: The South Indian Ocean Current. *J. Phys. Oceanogr.*, **22,** 421–430.

——, and R. G. Peterson, 1990: The South Atlantic Current. *J. Phys. Oceanogr.*, **20,** 846–859.

Streten, N. A., 1980: Some synoptic indices of the Southern Hemispheric mean sea level circulation 1972–77. *Mon. Wea. Rev.*, **108,** 18–36.

Szymanska, K., and M. Tomczak, 1994: Subduction of central water near the Subtropical front in the southern Tasman Sea. *Deep-Sea Res.*, **41,** 1373–1386.

Tsuchiya, M., 1982: On the Pacific upper-water circulation. *J. Mar. Res.*, **40,**(Suppl.), 777–799.

Warmus, K., 1989: Subtropical convergence: R. V. *Franklin* Cruise FR11/88—Data report. University of Sydney Ocean Sciences Institute Tech. Rep. 20.

Warren, B. A., 1973: Transpacific hydrographic sections at Lats. 43°S and 28°S: The SCORPIO-Expedition. II: Deep-Water. *Deep-Sea Res.*, **20,** 9–39.

Wyrtki, K., 1962a: Geopotential topographies and associated circulation in the western South Pacific Ocean. *Aust. J. Mar. Freshwater Res.*, **13,** 89–105.

——, 1962b: The subsurface water masses in the western South Pacific Ocean. *Aust. J. Mar. Freshwater Res.*, **13,** 18–47.

——, 1971: *Oceanographic Atlas of the International Indian Ocean Expedition.* National Science Foundation, Washington, D.C., 531 pp.

——, L. Magaard, and J. Hager, 1976: Eddy energy in the oceans. *J. Geophys. Res.*, **81,** 2641–2646.